Journal of Polymer Research (2021) 28: 235
https://doi.org/10.1007/s10965-021-02597-9

ORIGINAL PAPER

Structural, electrical and electrochemical studies of ionic liquid-based polymer gel electrolyte using magnesium salt for supercapacitor application

Ashish Gupta[1] · Amrita Jain[2] · S. K. Tripathi[3]

Received: 17 December 2020 / Accepted: 31 May 2021 / Published online: 3 June 2021

Abstract
In the present studies, the effect of ionic liquid 1-Ethyl-2,3-dimethylimidazoliumtetrafluoroborate (EDiMIM)(BF_4) on ionic conductivity of gel polymer electrolyte using poly(vinylidene fluoride-co-hexafluoropropylene) [PVdF(HFP)] and magnesium perchlorate [$Mg(ClO_4)_2$] as salt was investigated. The maximum room temperature ionic conductivity for the optimized system was found to be of the order of 8.4×10^{-3} S cm^{-1}. The optimized composition reflects Vogel-Tammann-Fulcher (VTF) behavior in the temperature range of 25 °C to 100 °C. The X-ray diffraction, Fourier transform infrared spectroscopy and scanning electron microscopy studies confirm the uniform blending of ionic liquid, polymer, and salts along with the enhanced amorphous nature of the optimized system. Dielectric and modulus spectra studies provide the information of electrode polarization as well as dipole relaxation properties of polymeric materials. The optimized electrolyte system possesses a sufficiently large electrochemical window of the order of 6.0 V with stainless steel electrodes.

Keywords Gel polymer electrolyte · Ionic liquid · Ionic conductivity · Temperature dependence · Supercapacitors

Introduction

From the last few decades, the demand for high-performance energy storage devices for practical applications in electronics, wearable devices etc. are increased. To design this flexible device, gel polymer electrolytes (GPE) plays a significant role. GPEs are ionically conducting membranes that can replace the conventional liquid electrolyte which is used as a separator in electrochemical devices [1, 2]. A good polymer electrolyte for energy storage devices particularly supercapacitors and batteries is the one which comprises properties like good ionic conductivity, high electrochemical stability window (ESW), proper interfacial contacts, good thermal and mechanical stability [3, 4]. Most of the above requirements are satisfied by using GPEs [5–7]. To design a novel polymer electrolyte, an effort has been put to increase the amorphicity in the polymer which in turn facilitates the fast ion motion while maintaining its mechanical stability [8, 9].

In the recent few years, there has been increasing a large interest in the ionic liquid (ILs) based polymer electrolytes for electrochemical applications. Ionic liquids (ILs) with ample available charged ion species, chemically stable over a practical range of temperature, non-hazardous and having low vapor pressure offer a better option for electrochemical double layer (EDL) capacitors [10, 11]. Generally, ionic liquids are molten salts which typically consist of cations and anions of dissimilar size. The physical properties of ILs like the relative size of ions and viscosity strongly affect the ionic conductivity of electrolyte which is one of the main parameters to design electrochemical devices [12, 13], as high viscosity of ILs lowers the power density of energy storage devices, particularly supercapacitors. Krause et al. [14] has reported that the mixture of 1-butyl-1-methylpyrrolidinium bis{(trifluoromethyl) sulfonyl}imide ([Pyrr14][TFSI]) and propylene carbonate (PC) exhibits higher conductivity and lower viscosity at 298 K than those of neat ([Pyrr14][TFSI]) and still the operating voltage was as high as 3.5 V. Similarly, high viscosity

✉ S. K. Tripathi
sktripathi@mgcub.ac.in

[1] Government Tulsi Degree College, Anuppur, Madhya Pradesh 484224, India

[2] Institute of Fundamental Technological Research, Polish Academy of Sciences, Adolfa Pawińskiego 5b, 02-106, Warsaw, Poland

[3] Department of Physics, School of Physical Sciences, Mahatma Gandhi Central University, Bihar- 845401, India

of commonly used ionic liquid such as $EMImBF_4$ (37.7 cP), $BMImBF_4$ (233 cP) and EMImTFSI (28 cP) reduce the conductivity of the gel polymer electrolyte which limit the performance of the devices [15]. Motivated by the above interesting studies by using an ionic liquid, in the present studies, 1-ethyl-2, 3-dimethylimidazoliumtetrafluoroborate (EDiMIM)(BF_4) was used. (EDiMIM)(BF_4) is chosen because of the small size of cations and high ionic conductivity which offers promising physicochemical properties and displays good performance as an electrolyte in terms of specific capacitance, energy density, and cycle life. The choice of host polymer determines whether the gel polymer electrolyte has an excellent matrix or not. Various polymers like polyacrylonitrile (PAN) [16, 17], polyethylene oxide (PEO) [18, 19], polymethylmethacrylate (PMMA) [20, 21], polyvinylidene fluoride (PVDF) [22] and poly (vinylidene fluoride-co-hexafluoropropylene) (PVDF-HFP) [23, 24] has been used. In the present studies, PVdF-HFP has been chosen because of its strong electron-withdrawing functional groups (-C-F-), high dielectric constant ($\varepsilon = 8.4$) which is suitable for the dissolution of magnesium salt to keep a high concentration of charge carriers. PVdF-HFP also contains more amorphous domains that are capable of trapping a large amount of liquid electrolyte and hence it is considered as one of the most promising polymer matrices for gel polymer electrolytes [24, 25].

Nowadays, the world is progressing towards high performance and environmentally friendly energy storage devices [26, 27]. It is also a known fact that lithium-ion is incorporated in most of the commercially available batteries because of its high capacity and excellent cycle life [3, 28, 29]. But the risk of limited lithium supply which results in its significant increase in the price cannot be ignored [2]. Consequently, its high time to develop long term sustainable solutions by using the materials which are abundantly available and at effective cost. There can be many alternatives like magnesium, sodium and calcium, but just like lithium, sodium metal also has a tendency to dendritic growth [7]. However, magnesium seems to be less prone to dendritic growth, which may be because of the lower self-diffusion barrier [8–10]. There are couple of advantages of using this light metals like natural abundance, low cost and safety. Moreover, magnesium ion is divalent and it accounts for a twofold increase in achievable energy density with respect to Li^+ ion or Na^+ ion for equal amount of reacted ions. Hence, in the present studies, magnesium ion based gel polymer electrolyte was developed.

In the present studies, gel polymer electrolytes using PVdF(HFP) as host polymer, ionic liquid, and magnesium perchlorate has been synthesized and optimized. The structural, electrical and electrochemical properties were discussed in detail in the result and discussion section. The synthesized polymer electrolyte was suitable for supercapacitor applications and it was already reported in our previous work [30].

Experimental

Preparation of gel polymer electrolytes

The ionic liquid 1-Ethyl-2,3-dimethylimidazoliumtetrafluoroborate (EDiMIM)(BF_4), host polymer poly(vinyldeneflouride-co-hexafluoropropylene) [PVdF (HFP)] (PVdF(HFP), average MW ~ 400,000), and the salt magnesium perchlorate $Mg(ClO_4)_2$ were obtained from Sigma Aldrich, propylene carbonate (PC) as plasticizer from Loba Chemie and acetonitrile (ACN) as an intermediate solvent from Merck, Germany was used to prepare ionic liquid-based gel polymer electrolyte films. All the chemicals were used without further purifications. All the experiments were carried out in ambient atmosphere. The ionic liquid-based gel polymer electrolyte films [PVdF(HFP)—(EDiMIM)(BF_4)—PC-$Mg(ClO_4)_2$] were prepared by using "Solution Cast" method. In the process, initially, the liquid electrolyte was prepared by dissolving different concentrations of magnesium salt, $Mg(ClO_4)_2$ in propylene carbonate (PC) at RT. The different weight percent of the polymer, PVdF(HFP) and (EDiMIM)(BF_4) were dissolved by using magnetic stirrer separately in common solvent acetonitrile (ACN) at 45 °C for ~ 7 to 8 h. The optimized composition of liquid electrolyte was then mixed with the optimized solution of PVdF(HFP)-(EDiMIM)(BF_4)-ACN in different weight ratios and stirred thoroughly for ~ 8 h at 70 °C. The final optimized composition was [{PVdF(HFP)—EDiMIM(BF_4)}(7:3)] (20 wt%)—[PC—$Mg(ClO_4)_2$ (0.3 M)] (80 wt%). The obtained viscous mixture was then cast over glass petri-dishes and allowed the films to dried slowly in room temperature, thereafter, free-standing gel polymer electrolyte films (400–500 μm) were obtained (Fig. 1).

Instrumentation details

X-ray diffraction (XRD) patterns of the synthesized films were recorded using Bruker D8 Advance diffractometer with Cu-Kα radiation over the Bragg angle (2θ) range of 10–60°. The scan rate was fixed at 5° min^{-1}. The surface morphology of the gel polymer electrolyte is studied with the help of a scanning electron microscope (JEOL JXA—8100 EPMA). Fourier transforms infrared (FTIR) spectra of the polymeric systems were recorded using Bruker vertex 70 spectrophotometers. The thermal analysis of the polymer gel systems was carried out by using differential scanning calorimetry (DSC) from -70 to 175 °C at a heating rate of 10 °C min-1 in presence of nitrogen atmosphere with the help of Mettler Toledo DSC 822E. The electrical conductivity of gel

Fig. 1 Photograph of optimized gel polymer electrolyte film

polymer electrolytes was measured by using complex impedance spectroscopic techniques and it is carried out using LCR Hi-Tester (HIOKI-3522–50, Japan) over the frequency range of 100 kHz to 1 Hz with a signal level of 10 mV. The samples were cut into the proper size and sandwiched between two stainless steel electrodes for taking the conductivity measurements. The ionic transport number and electrochemical stability of the gel polymer electrolytes were carried out by CHI 608C, CH Instruments, USA.

Results and discussion

Structural and morphological studies

Figure 2(a-c) depicts the XRD pattern of pure PVdF(HFP) films, polymer/ionic liquid blend film, and optimized GPE

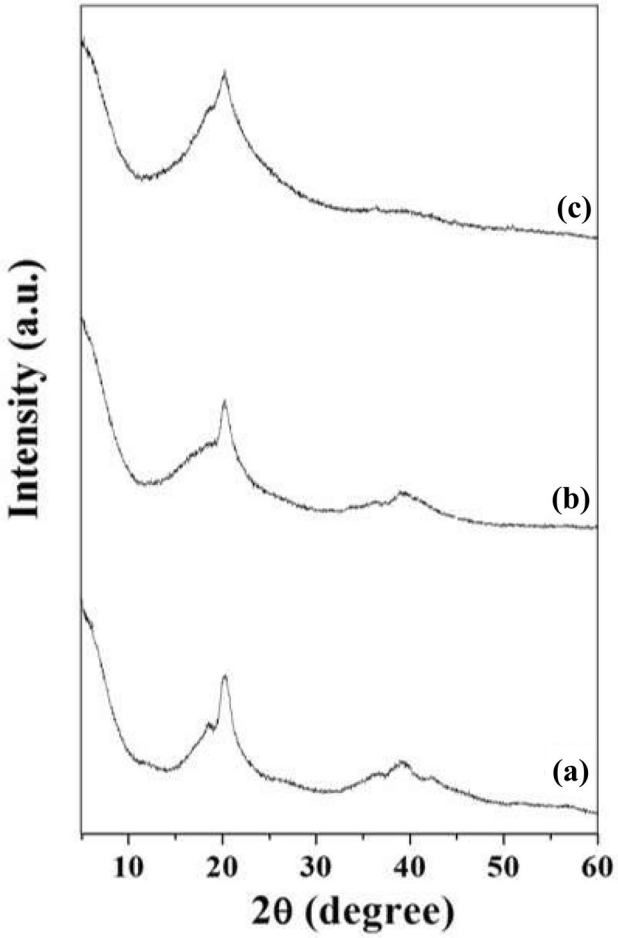

Fig. 2 XRD pattern of (**a**) Pure PVdF(HFP) film, (**b**) PVdF(HFP)-EDiMIM(BF_4) (7:3) polymer/ionic liquid blend, and (**c**) [{PVdF(HFP)-EDiMIM(BF_4)}(7:3)](20 wt%)-[PC-Mg(ClO_4)$_2$(0.3 M)](80 wt%) polymer gel

films. It can be seen from Fig. 2(a) that there exist predominant peaks at 2θ = 20.4° and 38° which corresponds to (020) and (021) crystalline peaks of PVdF(HFP) [31]. It confirms

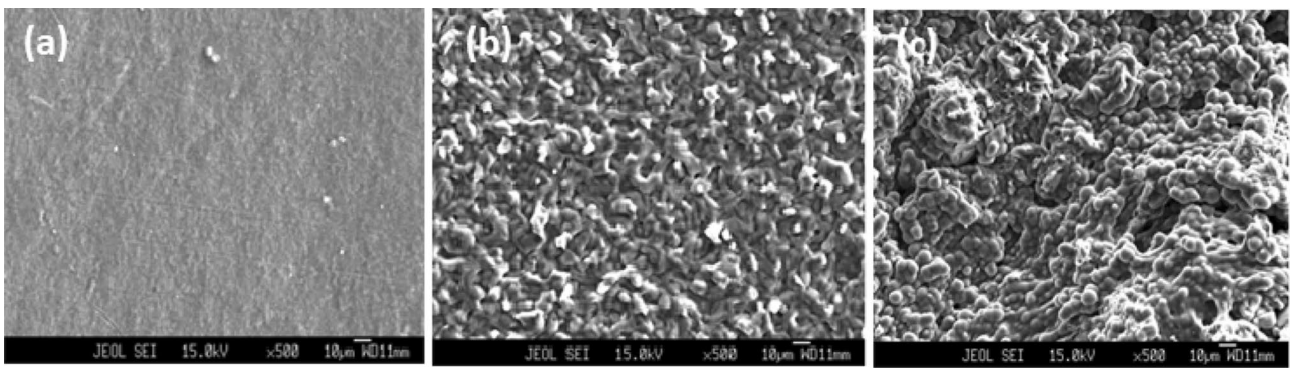

Fig. 3 (**a**-**c**): SEM image of (**a**) Pure PVdF(HFP) film, (**b**)[PVdF(HFP)-EDiMIM(BF_4)] (7:3) polymer/ionic liquid blend, and (**c**) [{PVdF(HFP)-EDiMIM(BF_4)}(7:3)](20 wt%)-[PC-Mg(ClO_4)$_2$ (0.3 M)] (80 wt%) gel polymer electrolytes

the partial crystallization of PVdF units and hence it shows the typical characteristics of a semi-crystalline morphology of the polymer, PVdF(HFP). Moreover, it is clear from Fig. 2(b), that when PVdF(HFP) is blended with the ionic liquid (EDiMIM)(BF_4), no additional peak appears, though the intensity of crystalline peak decreases and gets broadened, suggesting a decrease in the crystallinity of the blend system. Finally, when a liquid electrolyte is immobilized in the polymer/ionic liquid blend, the peak at $2\theta = 20°$ gets broadened and intense peak present at ~ 38° disappears, as can be seen from Fig. 2(c).

This suggests that the ionic liquid-based GPE is predominantly amorphous and its crystallinity gets depressed due to the proper immobilization and blending of liquid electrolyte in the optimized composition of polymer/ionic liquid blend systems at a molecular level. The amorphous nature of gel polymer electrolytes indicates an enhancement in its ionic conductivity, as it is well known that the ionic conduction occurs mainly through the amorphous phase of the polymeric system [31, 32].

Figure 3(a-c) shows the surface morphologies of pure PVdF(HFP) film, PVdF(HFP)/(EDiMIM)(BF_4) blend film and optimized GPE film. Figure 3(b) shows the interconnected and uniformly distributed pore structure of the blend system, which can retain the liquid electrolytes solution in them. Further as can be seen from Fig. 3(c) that after addition of liquid electrolytes, homogeneously distributed pore morphology is observed which is capable for the better ion transport through the polymer chain/network of the optimized composition of GPE system which is suitable for energy storage devices like supercapacitors.

Thermal properties of gel polymer electrolytes were carried out by using differential scanning calorimetry (DSC) technique. DSC studies also confirm the proper blending of electrolyte films. The DSC profile of the pure PVdF(HFP) film, different weight ratios of polymer/ionic liquid blend films PVdF(HFP)-EDiMIM(BF_4) and optimized composition of gel polymer electrolyte films are shown in Fig. 4(a-d). The endothermic peak at ~ 142 °C corresponds to the melting point of pure polymer PVdF(HFP). From Fig. 4(b) and (c), it can be seen that the melting point of polymer/ionic liquid blend systems PVdF(HFP)-EDiMIM(BF_4) reduces

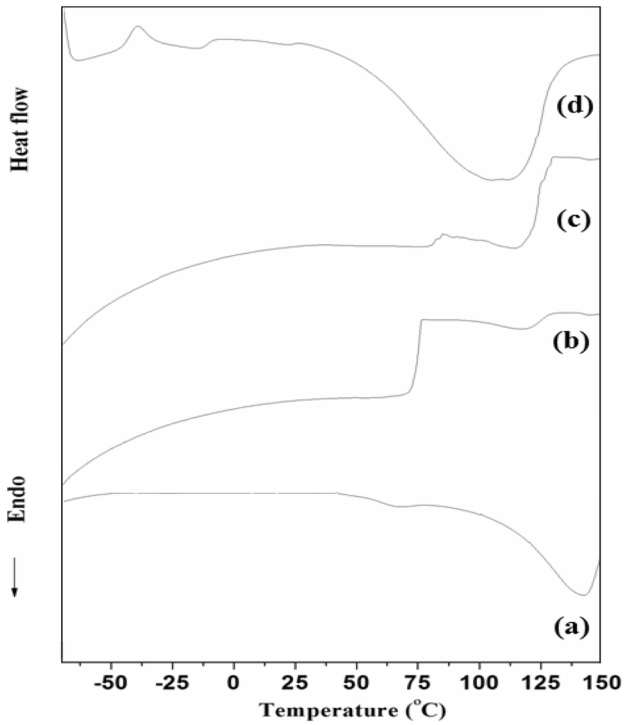

Fig. 4 DSC profile of (**a**) pure PVdF(HFP) film, (**b**) polymer/ionic liquid blend film [PVdF(HFP): EDiMIM(BF_4)] (7:3), (**c**) [PVdF(HFP): EDiMIM(BF_4)] (6:4), and (**d**) gel polymer electrolytes film [{PVdF(HFP): EDiMIM(BF_4)} (7:3)](20 wt%)-[{PC-Mg(ClO_4)$_2$} (0.3 M)](80 wt%)

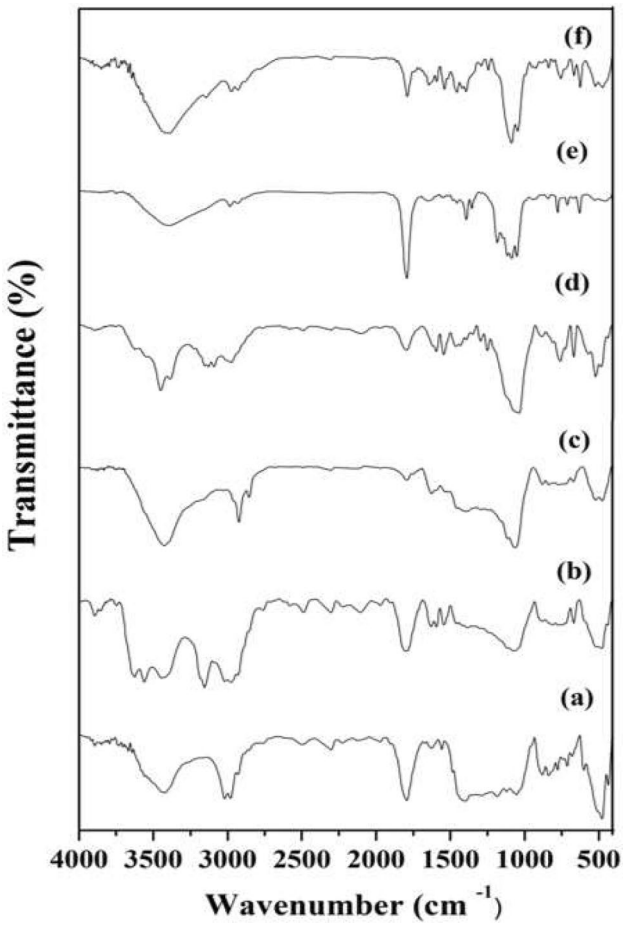

Fig. 5 FTIR Spectra of (**a**) Pure PVdF(HFP) film, different ratios of polymer/ionic liquid blend films (**b**) [PVdF(HFP)-EDiMIM(BF_4)] (8:2), (**c**) [PVdF(HFP)-EDiMIM(BF_4)](7:3), (**d**) [PVdF(HFP)-EDiMIM(BF_4)] (6:4) and polymer gel electrolyte films in different ratios of (**e**) [{PVdF(HFP)-EDiMIM(BF_4)}(7:3)](20 wt%)-[PC-Mg(ClO_4)$_2$ (0.3 M](80 wt%) (**f**) [{PVdF(HFP)-EDiMIM(BF_4)}(7:3)] (30 wt%)—[PC-Mg(ClO_4)$_2$ (0.3 M)] (70 wt%)

to ~ 118 °C for (7:3) ratio and ~ 116 °C for (6:4) ratio respectively. On addition of optimized composition of liquid electrolyte in blend system, its melting point further decreases to ~ 105 °C, which is the indication of proper interaction of polymer, ionic liquid and salts in gel polymer electrolyte system [PVdF(HFP)-EDiMIM(BF_4)-PC-Mg(ClO_4)$_2$].

The existence of a broader and asymmetrical melting peak indicates the entrapment of the appreciable amount of liquid electrolyte components in the polymer matrix, which causes the enhancement of amorphous content of the gel polymer electrolyte systems and thereby increasing its electrical conductivity accordingly (also confirmed from SEM studies). The sharp peak at about -38 °C has been observed in GPE as can be seen from Fig. 4(d), which indicates the presence of another separate crystalline phase due to the possible interaction of EDiMIM(BF_4) with polar PVdF(HFP).

Figure 5(a-f) shows the comparative FTIR spectra of pure PVdF(HFP), polymer-ionic liquid PVdF(HFP)- (EDiMIM)(BF_4) blend films, PVdF(HFP)-(EDiMIM)(BF_4)-PC-Mg(ClO_4)$_2$ polymer gel electrolytes film in the wavenumber region varying from 450–4000 cm^{-1}. It was mainly performed to visualize the interaction of Mg^{2+} ion and ionic liquid with the host polymer PVdF(HFP) at a microscopic level in the optimized gel polymer electrolyte. It also throws light on the conformational changes by the entrapment of liquid electrolyte PC-Mg(ClO_4)$_2$ and ionic liquid (EDiMIM)(BF_4) in the polymer matrix.

From Fig. 5(a), it is clear that the spectrum of pure PVdF(HFP) contains the vibrational band at wavenumbers 478, 669, 772, 837, 880, 1185 and 1793 cm^{-1} that corresponds to vinylidene group, CF_2 bending of the vinylidene band, CF_3 deformation vibration, C(F)-C(H)-C(F) skeletal bending vibration, CH_2 wagging vibration of vinylidene band, out-of-plane C-H bending, -C-F- stretching and $CF=CF_2$ stretching vibration of the vinylidene groups respectively [33–35], the important bands are summarized in Table 1. The higher frequencies of 3020 and 2986 cm^{-1}, it is assigned to CH_2 asymmetric and symmetric stretching vibration respectively (Table 1).

Figure 5(b-d) shows some additional bands at 1074, 1545, 1593, and 1635 cm^{-1}, which confirms that ionic liquid is well blended with the host polymer at a molecular

Table 1 Assignment of important FTIR bands of pure PVdF(HFP), polymer/ionic liquid blend (PVdF(HFP) (EDiMIM (BF_4) and optimized gel polymer electrolytes

Band Assignment	PVdF(HFP) film	[PVdF(HFP)-EDiMIM(BF_4] (8:2)	[PVdF(HFP)-EDiMIM(BF_4] (7:3)	[PVdF(HFP)-EDiMIM(BF_4] (6:4)	[{PVdF(HFP)-EDiMIM(BF_4)} (7:3)] (20 wt%)- [PC-($MgClO_4$)$_2$ (0.3 M)] (80 wt%)	[{PVdF(HFP)-EDiMIM(BF_4}] (7:3) (30 wt%)- [PC-($MgClO_4$)$_2$ (0.3 M)] (70 wt%)
O–H stretching vib	3418	3444	3426	3449	3413	3415
CH_2 asymmetric stretching vib	3020	3027	-	3017	-	-
CH_2 symmetric stretching vib	2986	2976	-	2969	2984	2984
-$CF=CF_2$ stretching vib	1793	1798	1798	1793	1792	1789
C-N vibration of aromatic ring (IL)	-	1635	1627	-	1651	1644
C=C stretch vib. (IL)	-	1593	-	1595	-	1587
N–H bending vib. (IL)	-	1545	-	1547	1547	1538
- C-F- stretching vib	1185	-	-	-	1184	-
CH_2(N) bending		1074	1064	1069	1064	1068
C=O stretching (PC)	-	-	-	-	1052	1051
C-O stretching vib. (PC)	-	-	-	-	930	928
C-H out of plane	880	880	887	882	-	879
CH_2 wagging vib	837	836	835	-	842	837
C(F)-C(H)-C(F) skeletal bending vib	772	772	-	777	777	797
CF_3 deformation vib	669	669	663	668	663	666
ClO_4^- ion pair					630	627
CF_2 bending	478	479	470	479	455	475

level. The bands at 1074 and 1545 cm^{-1} corresponds to the $EDiMIM^+$ peak and are assigned for $CH_2(N)$ bending, N–H bending vibrations respectively [36–38]. The peaks observed at 1593 and 1635 cm^{-1} are attributed to the C = C and C-N stretching vibrations of imidazolium cation.

Further, in Fig. 5(e–f), bands at 1052, 930 and 627 cm^{-1} were observed and it is due to the presence of plasticizer (PC) and anion $(ClO_4)^-$ in the ionic liquid-based gel polymer electrolytes. The vibrational bands at 1052 and 930 cm^{-1} are assigned to the C = O stretching and C-O stretching of the plasticizer (PC) [39]. The vibrational frequency at 627 cm^{-1} is attributed to the ion-pairing of $(ClO_4)^-$ anions [40, 41]. The increased or decreased pattern of frequency shifting peaks from pure PVdF(HFP) spectra shows the strong interactions of polymer with the ionic liquid and liquid electrolytes respectively in the ionic liquid-based gel polymer electrolytes. However, disappearance of bands associated with crystalline α-phase and broadening of the band of amorphous phase of the polymer indicate a decrease in crystallinity and the increment of amorphous phase in gel polymer electrolyte system which is advantageous from application point of view.

Electrical and electrochemical properties

The optimization and room temperature ionic conductivity of [{PVdF(HFP)-EDiMIM(BF_4)(7:3)}(20 wt%)-{PC-Mg(ClO_4)$_2$}(80 wt%)] polymer electrolyte system has summarized in Table 2 and the detail discussion and analysis are reported in our previous work [30].

Temperature dependence conductivity studies of the optimized composition of gel polymer electrolytes are shown in Fig. 6 and it reflects the nonlinear behavior and following the Vogel-Tammann-Fulcher (VTF) [43] characteristics of the system which can be expressed as:

$$\sigma = AT^{-1/2} exp\left(\frac{-B}{T - T_0}\right) \quad (1)$$

where the parameter B has a dimension of energy and is related to the critical free volume for ion transport, A is a pre-exponential factor, which represents the conductivity at infinitely high temperature and T_0 is equilibrium glass transition temperature close to the T_g values. These parameters have been evaluated by the non-linear least-squares fitting of the data and are enlisted in Table 3. The increase in the conductivity with the temperature of the gel polymer electrolytes can be explained based on the free volume mechanism as proposed by Kim et.al. [42].

According to this concept, such behavior is observed due to the hopping mechanism between coordinating sites and segmental motion of the polymer matrix. With the increase in temperature amorphous nature increases which is favorable for the hopping of ions within a polymeric network from one chain to another and leads to the enhancement in ionic conductivity [43, 44]. It can also be observed from the plot that the optimized composition of gel polymer electrolyte shows electrical conductivity of the order of ~ 10^{-3} S cm^{-1} at room temperature (~ 25 °C) and the order of ~ 10^{-2} S cm^{-1} at 100 °C, showing a span of wider temperature range which is beneficial for temperature dependence electrochemical devices.

Dielectric studies were also carried out to study the ionic transport phenomenon of ionic liquid-based gel polymer electrolyte system [45]. The real (ε_r) and imaginary part (ε_i) of dielectric studies provide information about the storage and loss of energy in every cycle of the applied electric field. Figure 7(a-b) shows the dielectric constant (ε_r) and dielectric loss (ε_i) as a function of frequency at different temperatures for an optimized system. From Fig. 7(a) it can be seen that the values of ε_r is rising very sharply towards low-frequency region, which can be explained based on the electrode polarization effect [46]. This low-frequency dispersion region is attributed to the high contribution of charge accumulation

Table 2 Electrical conductivity of optimized ionic liquid electrolyte, polymer/ionic liquid blend, optimized gel polymer electrolytes

Material	σ(Scm^{-1}) at room temperature (~ 25 °C)
PC- Mg(ClO_4)$_2$ (0.3 M)	3.63×10^{-3}
PVdF(HFP) (70 wt%)—EDiMIM(BF_4) (30 wt%)	4×10^{-5}
[PVdF(HFP)-EDiMIM(BF_4)(7:3)] (20 wt%)—[PC—Mg(ClO_4)$_2$ (0.3 M)] (80 wt%)	8.4×10^{-3}

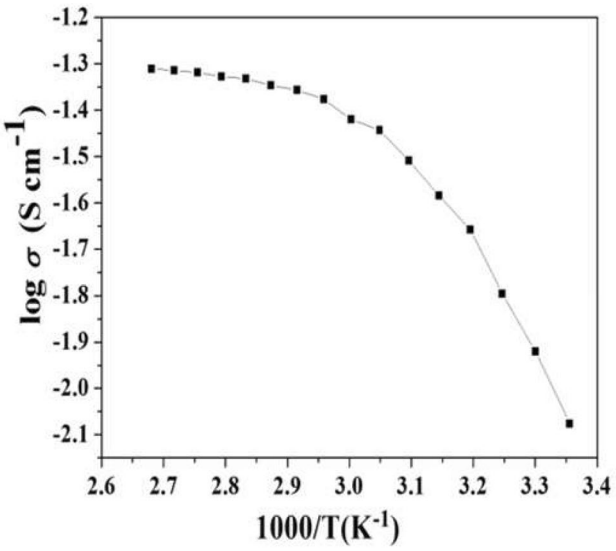

Fig. 6 Variation of electrical conductivity of optimized gel polymer electrolytes as a function of temperature

Table 3 Different parameter (A, B and T_0) for ionic liquid-based gel polymer electrolyte obtained by nonlinear least-square fitting of conductivity data to VTF equation

Sample	Parameters		
	A(S cm^{-1}) K$^{-1/2}$	B(eV)	T_0(K)
[PVdF(HFP)-EDiMIM(BF_4)(7:3)] (20 wt%)—[PC—Mg(ClO_4)$_2$ (0.3 M)] (80 wt%)	0.1257	0.33	286

at the electrode–electrolyte interfaces. In higher frequency regions it was found that the value of ε_r is almost constant with frequency. It happens so because the periodic reversal of the electric field occurs so fast that the charge carriers will not get sufficient time to orient themselves in the field direction. Hence there is no excess ion diffusion in the direction of the field and it further leads to the decrease in the values of dielectric constant [47]. Again, from Fig. 7(b), it can be seen that the dielectric loss (ε_i) becomes very large towards the lower frequency region. It is due to the motion of free charge carriers within the material.

Modulus spectroscopy studies were carried out to understand the bulk properties of the materials which gives the insight of electrode and grain boundaries effect. Figure 8 (a-b) shows the real part (M_r) and the imaginary part (M_i) of electrical modulus as a function of frequency at various temperatures for gel polymer electrolytes. It has been observed that the values of M_r and M_i were increased in the high-frequency region and provide a long tail towards lower frequency. The peaks in the modulus formalism at higher frequencies show that the gel polymer electrolyte films are predominantly ionic conductors [48]. It has also been observed from the plots that the values of M_r and M_i decrease towards lower frequencies; it might be because of the electrode polarization phenomenon which makes a negligible contribution, and its effect seems to be vanishing towards lower frequency domain. The increasing peak of Fig. 8(b) can be related to the translational ion dynamics and mirrors the conductivity relaxation of the mobile ions. The shapes of all the plots are identical for all temperatures and show a single relaxation peak in the range of temperature and frequency determined under present studies. The angular frequency,ω_c at which the maximum Mi occurs represents the relaxation time, τ_c and are related to each other by a mathematical $\tau_c\omega_c = 1$ [49]. Further, it is also observed that M_i shows a slightly asymmetric peak at each temperature. The peak shifts towards higher frequency regions with increasing temperature. The broad nature of peaks can be understood as being the result of distributions of relaxation time. These peaks are broader than the Debye peak, which is treated as an ideal ionic conductor represented by a single parallel RC element.

Figure 9 shows the conductance spectra for ionic liquid-based gel polymer electrolytes, [PVdF(HFP)-EDiMIM(BF_4)- PC-Mg(ClO_4)$_2$ at different temperatures. The spectra consist of two regions, a low-frequency dispersive region due to electrode–electrolyte interfacial phenomena and the plateau region representing the dc conductivity. As the frequency decreases, more and more charge accumulation occurs at the electrode–electrolyte interfaces which lead to a decrease in the number of mobile ions and eventually to a drop in conductivity towards lower frequency

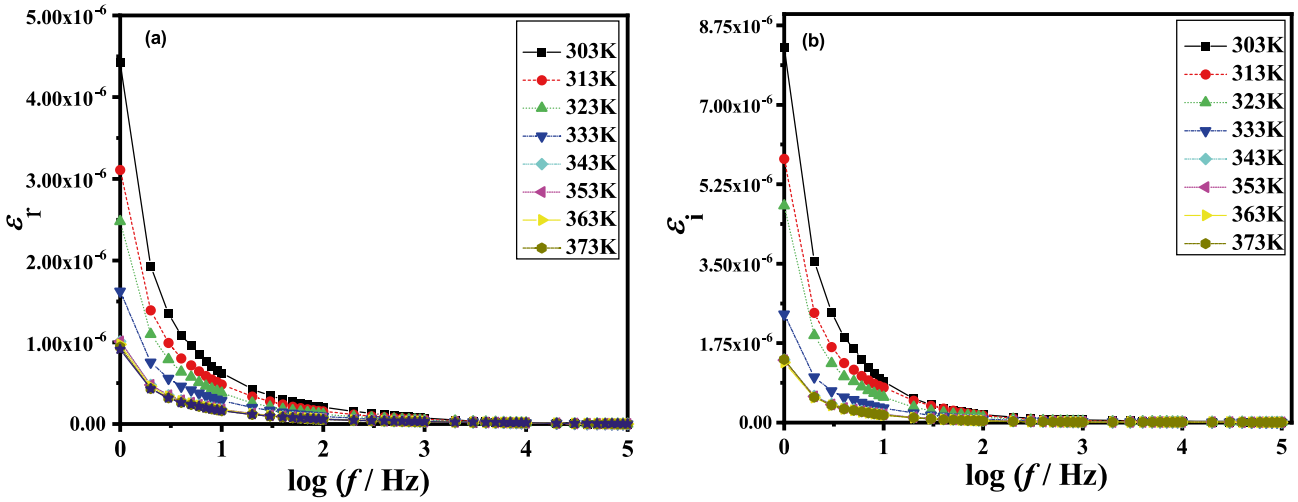

Fig. 7 (**a**) Variation of dielectric constant of gel polymer electrolytes system as a function of frequency at various temperature and (**b**) Variation of dielectric loss of gel polymer electrolytes system as a function of frequency at various temperatures

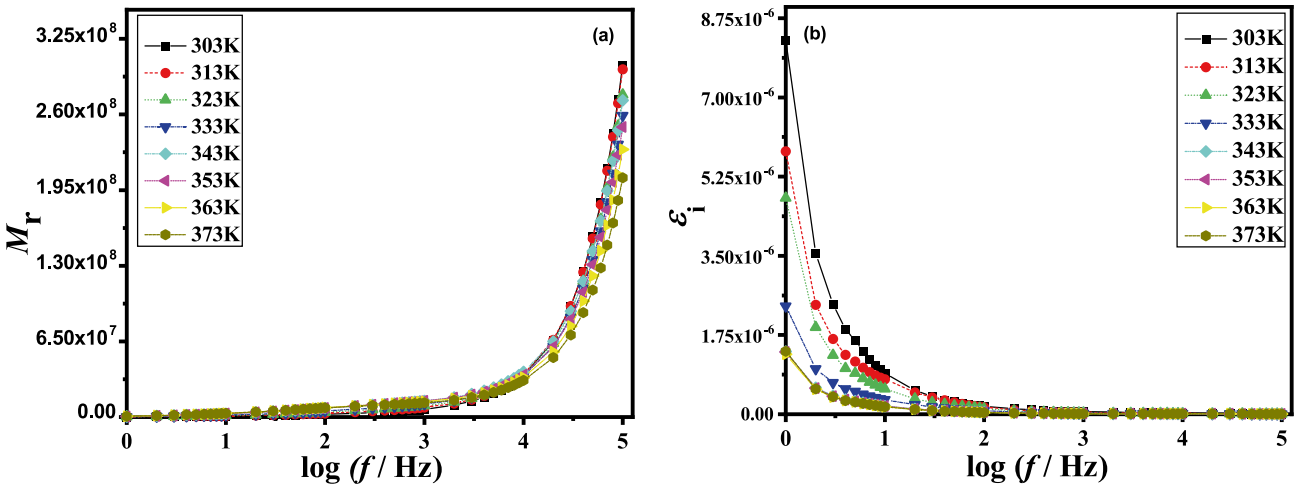

Fig. 8 (**a**) Variation of real part of modulus of gel polymer electrolytes as function of frequency at various temperature and (**b**) Variation of imaginary part of modulus of gel polymer electrolytes as a function of frequency at various temperatures

region. In the high-frequency region, the mobility of charge carriers is high and hence the conductivity increases with frequency [50, 51]. It has been observed that the dc conductivity increases with temperature which suggests that the free volume around the polymer chain causes the mobility of ions and polymer segments. The phenomenon of the conductivity dispersion is generally represented by Jonscher's law [50].

Mathematically it can be written as $\sigma(\omega) = \sigma_{dc} + A\ \omega^n$, where σ_{dc} is the direct current (dc) conductivity of the sample, A is a constant for a particular temperature and n is the frequency exponent lying in between the range of $0 < n < 1$. The values of n represent the degree of interaction between the mobile ions and the environments surrounding them. For ionic conductors this value lies between 0.5 and 1, indicating the ideal long-range pathway diffusion of the ions and

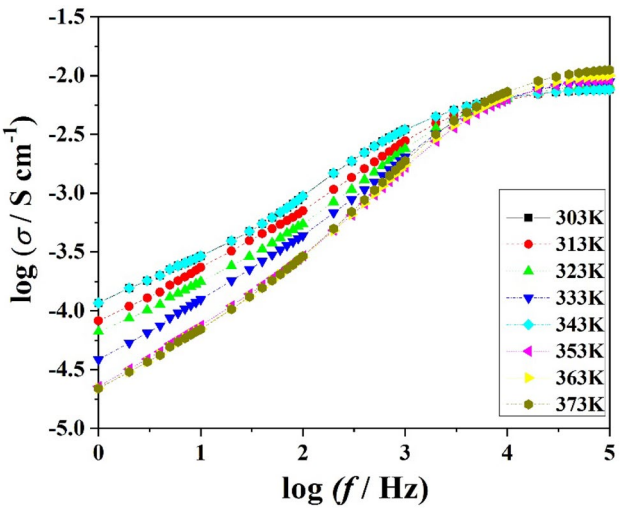

Fig. 9 Variation of ionic conductivity as a function of frequency with temperature for gel polymer electrolytes system

can be best explained by hopping models [52]. When the value of $n = 0$, the motion is completely random and independent Debye like ion hopping mechanism is taking place in the system. The high probability of forward–backward hopping at higher frequencies together with the relaxation of the dynamic cage potential is mainly responsible for the observation of high-frequency dispersion in its conductivity.

The relaxation phenomenon of any gel polymer electrolyte materials can be described by its dielectric tangent loss (tan δ). It provides information about the energy lost or dissipated per cycle to the energy stored. Figure 10 shows the plot of tangent loss as a function of frequency at different temperature for the optimized polymer gel electrolytes, [{PVdF(HFP)-EDiMIM(BF_4)}(7:3)](20 wt%)-[{PC-Mg(ClO_4)$_2$}(0.3 M)](80 wt%).

It is observed from the plot that the general trend shows the increase in the values of loss tangent with increasing frequency at different temperatures, thereafter it passes through its maxima and finally decreases. Further, it can be seen that by increasing the temperature, the values of loss tangent maxima and peak intensity get shifted towards a higher frequency side. This phenomenon can be understood in terms of relaxation due to the ionic transport processes of the bulk and the grain boundaries [52–54].

The linear sweep voltammogram (LSV) curves are recorded for the optimized system at a scan rate of 5 mV s^{-1} and is depicted in Fig. 11. The working voltage range of the electrochemical device is strongly dependent on the potential window of the GPEs. This is a very important parameter that gives the optimum voltage stability range of the electrolyte materials from the application point of view. In the present studies, the electrochemical stability of polymer gel electrolyte has been measured using linear sweep cyclic voltammetry, by sandwiching the gel electrolytes in

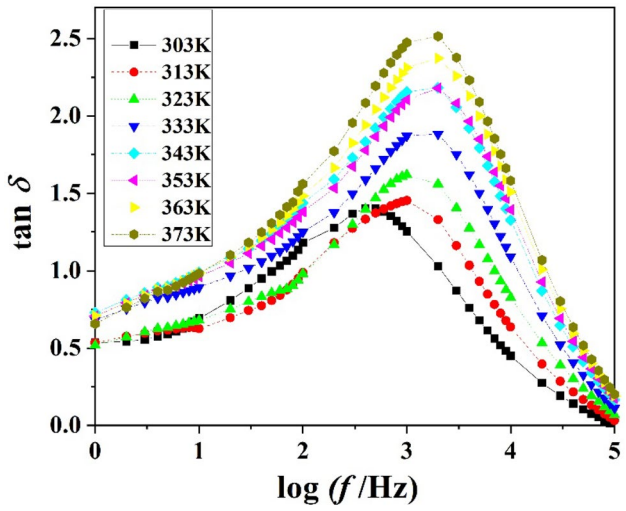

Fig. 10 Variation of loss tangent (tan δ) as a function of frequency at different temperature for gel polymer electrolytes

between two stainless steel (SS) electrodes. From the figure, it can be seen that the current values increase gradually by an increase in applied voltage across the cell up to a certain voltage and thereafter it increases abruptly. The sudden increase in the value of current shows the decomposition of the electrolyte materials; hence the values of the potential window provide information about the polymeric system up to which it can work safely. In the present studies, ionic liquid-based gel polymer electrolytes show the potential window of ~ 6.0 V, which represents the potential limit up

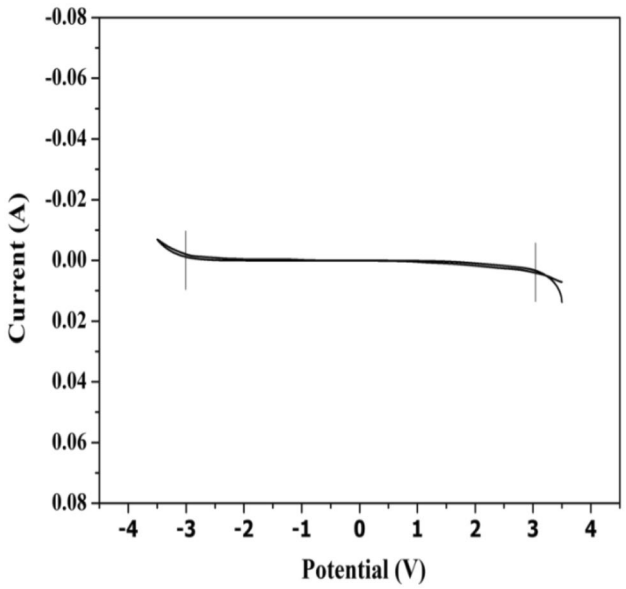

Fig. 11 Linear sweep cyclic voltammetry curves of gel polymer electrolytes cell SS| PGE|SS recorded at room temperature at a scan rate 5 mV s^{-1}

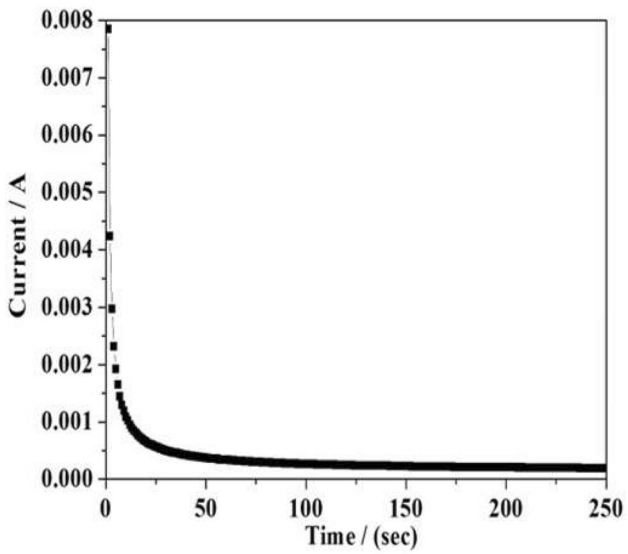

Fig. 12 dc polarization curve as a function of time for polymer gel electrolyte

to which any electrochemical device using this electrolyte can work safely without decomposition.

The ionic transport number of gel polymer electrolyte in the present studies has also been calculated by using dc polarization method. Figure 12 shows the dc polarization curve of gel polymer electrolytes, sandwiched between symmetrical SS electrodes. In this method, a typical cell SS | [{PVdF(HFP)-EDiMIM(BF_4)} (7:3)] (20 wt%—[{PC-$Mg(ClO_4)_2$} (0.3 M)](80 wt%) | SS is being polarized by applying a potential of 1.0 V and its corresponding current has been measured as a function of time. The value of the ionic transport number is found to be 0.97 which confirms that the overall conductivity of ionic liquid-based gel polymer electrolytes using magnesium salt is predominantly ionic.

The optimized system is already tested for supercapacitor application by using activated charcoal as an electrode material. In that paper, we have reported very promising results like capacitance value of 868 mF cm^{-2} with energy density of 55 Wh kg^{-1} and power density of 2 kW kg^{-1} has been achieved by using activated carbon as electrode with present electrolyte films [30].

Conclusions

An ionic liquid-based and magnesium ion conducting gel polymer electrolyte were prepared and its structural, electrical and electrochemical properties were discussed in detail. It was observed that 20 wt % of polymer/ionic liquid blend, PVdF(HFP)-EDiMIM(BF_4) (7:3) is optimized for the synthesis of gel polymer electrolytes having an electrical conductivity

of the order of 8.4×10^{-3} S cm^{-1} at room temperature with acceptable mechanical stability. The SEM and XRD studies confirm the porous and predominantly amorphous nature of the prepared electrolyte material along with the good liquid retention capability which supports the electrical conductivity through its polymer matrix.

FTIR studies show the proper interaction of polymer, ionic liquid and liquid electrolytes at a microscopic level.

The temperature dependence studies for electrical conductivity (σ) show the VTF behavior of the gel polymer electrolytes and its activation energy has been evaluated by the non-linear least squares curve fitting of the data and it is found to be of the order of $E_a = 0.33$ eV. The highest conducting composition carries a significant electrochemical stability window of ~ 6.0 V which confirms its suitability for electrochemical applications. The ionic transport number for GPE is 0.97, which shows that the charge transport mechanism is predominantly ionic. Dielectric and modulus spectra studies provides the information of electrode polarization as well as dipole relaxation properties of polymeric materials. As it has been mentioned earlier that the electrolyte material was suitable for supercapacitor application using activated carbon as electrode material.

Acknowledgements The authors are grateful to the Madhya Pradesh Council of Science and Technology, Madhya Pradesh, India for providing financial support to Prof. S.K. Tripathi through Grant-in-Aid for Scientific Research vide sanction no. [3683/CST/R&D/Phy & Engg. Sc/2012; Bhopal, Dated: 03.11.2012]. Authors are also thankful to Jaypee University of Engineering and Technology, Guna, India for providing electrochemical and electrical characterization facilities. We are also thankful to Dr. J.K. Bera, Department of Chemistry, IIT Kanpur for providing FTIR facilities, Dr. Kamlesh Pandey, NCEMP, Allahabad for providing SEM facilities, Dr. Ajay Gupta and Dr. Mukul Gupta, UGC-DAE Consortium for Scientific Research, Indore-center for providing the XRD facility and STIC, Cochin University, Kerala, for DSC measurement.

Author's Contribution Ashish Gupta: Investigation, Validation, Software, Formal analysis. Writing-Original Draft. Amrita Jain: Conceptualization, Data curation, Writing-Original Draft, Visualization. S.K. Tripathi: Conceptualization, Supervision, Writing-Review & Editing, Funding acquisition.

References

1. Fang J, Qiao J, Wilkinson DP, Zhang J (2017) Electrochemical Polymer Electrolyte Membranes. CRC Press
2. Zhang P, Li R, Huang J, Liu B, Zhou M, Wen B, Xia Y, Okada S (2021) Flexible poly(vinylidene fluoride-co-hexafluoropropylene)-based gel polymer electrolyte for high-performance lithium-ion batteries. RSC Adv 11:11943–11951
3. Famprikis T, Canepa P, J. A. Dawson JA, Islam MS, Masquelier C, (2019) Fundamentals of inorganic solid-state electrolytes for batteries. Nat Mater 18:1278–1291
4. Hashmi SA, Yadav N, Singh MK (2020) Polymer Electrolytes for Supercapacitor and Challenges. Characterization Techniques and Energy Applications. Wiley-VCH Verlag GmbH & Co. KGaA, Polymer Electrolytes, pp 231–297
5. Jin M, Zhang Y, Yan C, Fu Y, Guo Y, Ma X (2018) High-Performance Ionic Liquid-Based Gel Polymer Electrolyte Incorporating Anion-Trapping Boron Sites for All-Solid-State Supercapacitor Application. ACS Appl Mater Interfaces 10:39570–39580
6. Bhat Y, Yadav N, Hashmi SA (2020) Gel Polymer Electrolyte Composition Incorporating Adiponitrile as a Solvent for High-Performance Electrical Double-Layer Capacitor ACS Appl. Energy Mater 3:10642–10652
7. Beenarani BB, Sugumaran CP (2021) The Electrochemical Performance of Simple, Flexible and Highly Thermally Stable PVA-TiO_2 Nanocomposite in an All-Solid-State Supercapacitor IEEE Trans Nanotechnol 20:215–223
8. Gray FM (1991) Solid Polymer Electrolytes-Fundamental and Technological Applications. Wiley, New York, NY, USA
9. Narayanagari R, Vukka R, Chekuri R (2021) Preparation and characterization of titanium oxide based poly (vinylidene fluoride-co-hexafluoropropylene) polymer electrolyte films. J Polym Res 28:4
10. Samui AB, Sivaraman P (2010) Polymer Electrolytes: Fundamentals and Applications, Science Direct
11. Eftekhari A (2017) Supercapacitors utilizing ionic liquids. Energy Storage Mater 9:47–69
12. Obeidat AM, Luthra V, Rastogi AC (2019) Solid-state graphene-based supercapacitor with high-density energy storage using ionic liquid gel electrolyte: electrochemical properties and performance in storing solar electricity. J Solid State Electr 23:1667–1683
13. Khosrozadeh A, Xing M, Wang Q (2015) A high-capacitance solid-state supercapacitor based on the free-standing film of polyaniline and carbon particles. Appl Energy 153:87–93
14. Pal P, Ghosh A (2018) Solid-state gel polymer electrolytes based on ionic liquids containing imidazolium cations and tetrafluoroborate anions for electrochemical double-layer capacitors: Influence of cations size and viscosity of ionic liquids. J Power Sources 406:128–140
15. Krause A, Balducci A (2011) High voltage electrochemical double-layer capacitor containing mixtures of ionic liquids and organic carbonate as electrolytes. Electrochem Commun 13:814–817
16. Zhang Q, Yang H, Lang X, Zhang X, Wei Y (2019) 1-Ethyl-2,3-dimethyl imidazolium tetrafluoroborate ionic liquid mixture as an electrolyte for high-voltage supercapacitors. Ionics 25:231–239
17. Fan X, Liu J, Ding J, Deng Y, Han X, Hy W, Zhong C (2019) Investigation of the Environmental Stability of Poly(vinyl alcohol)–KOH Polymer Electrolytes for Flexible Zinc-Air Batteries. Front Chem 7:678
18. Zeng F, Sun Y, Hui B, Xia Y, Zou Y, Zhang X, Yang D (2020) Three-Dimensional Porous Alginate Fiber Membrane Reinforced PEO-Based Solid Polymer Electrolyte for Safe and High-Performance Lithium Ion Batteries ACS Appl. Mater Interfaces 12:43805–43812

19. Feng J, Wang L, Chen Y, Wang P, Zhang H, He X (2021) PEO based polymer-ceramic hybrid solid electrolytes: a review Nano Converg 8:2
20. Meabe L, Huynh TV, Mantione D, Porcarelli L, Li C, O'Dell LA, Sardon H, Armand M, Forsyth M, Mecerreyes D (2019) UV-cross-linked poly(ethylene oxide carbonate) as free standing solid polymer electrolyte for lithium batteries. Electrochim Acta 302:414–421
21. Mathew CM, Kesavan K, Rajendran S (2015) Structural and Electrochemical Analysis of PMMA Based Gel Electrolyte Membranes. Int J Electrochem Volume 2015, Article ID 494308 7 pages
22. Tripathi SK, Gupta A, Kumari M (2012) Studies on electrical conductivity and dielectric behavior of PVdF–HFP–PMMA–NaI polymer blend electrolyte. Bull Mater Sci 35:969–975
23. Xu P, Chen H, Zhou X, Xiang H (2021) Gel polymer electrolyte based on PVDF-HFP matrix composited with rGO-PEG-NH2 for high-performance lithium ion battery. J Membr Sci 617:118660
24. Tripathi SK, Jain A, Gupta A, Mishra M (2012) Electrical and electrochemical studies on magnesium ion-based polymer gel electrolytes. J Solid State Electr 16:1799–1806
25. Chen G, Zhang F, Zhou Z, Li J, Tang Y (2018) A Flexible Dual-Ion Battery Based on PVDF-HFP-Modified Gel Polymer Electrolyte with Excellent Cycling Performance and Superior Rate Capability. Adv Energy Mater 8:1801219
26. Perdana YS, Muyeen SM, Al-Durra A, Morales-Paredes HK, Simões MG (2018) Direct Connection of Supercapacitor-Battery Hybrid Storage System to the Grid-Tied Photovoltaic System. IEEE Trans Sustain Energy 10:1370–1379
27. Zhang Q, Li G (2020) Experimental Study on a Semi-Active Battery-Supercapacitor Hybrid Energy Storage System for Electric Vehicle Application. IEEE Trans Power Electron 35:1014–1021
28. Mauger A, Julien CM, Paolella A, Armand M, Zaghib K (2018) A comprehensive review of lithium salts and beyond for rechargeable batteries: Progress and perspectives. Mater Sci Eng R Rep 134:1–21
29. Ravada BR, Tummuru NR (2020) Control of a Supercapacitor-Battery-PV Based Stand-Alone DC-Microgrid IEEE T Energy Conver 35:1268–1277
30. Jain A, Tripathi SK, Gupta A, Kumari M (2013) Fabrication and characterization of electrochemical double-layer capacitors using ionic liquid-based gel polymer electrolyte with chemically treated activated charcoal electrodes. J Solid State Electr 17:713–726
31. Solarajan AK, Murugadoss V, Angaiah S (2017) High performance electrospun PVdF-HFP/SiO2 nanocomposite membrane electrolyte for Li-ion capacitors. J Appl Polym Sci 134:45177
32. Panero S, Satolli D, D'Epifano A, Scrosati B (2002) High voltage polymer cells using a PAN based composite electrolyte. J Electrochem Soc 149:A414–A417
33. Deka M, Kumar A (2009) Ionic transport in (PVdF-HFP)-PEO based novel microporous polymer electrolytes. Bull Mater Sci 32:627–632
34. Li Z, Su G, Gao D, Wang X, Li X (2004) Effect of Al_2O_3 nanoparticles on the electrochemical characteristics of P(VDF-HFP)-based polymer electrolyte. Electrochim Acta 49:4633–4639
35. Shukla N, Shukla A, Thakur AK, Choudhary RNP (2008) Low temperature ferroelectric behavior of PVDF based composites. Indian J Eng Mater S 15:126–132
36. Kiefer J, Fries J, Leipertz A (2007) Experimental Vibrational Study of Imidazolium-Based Ionic Liquids: Raman and Infrared Spectra of 1-Ethyl-3-methylimidazolium Bis(trifluoromethylsulfonyl)imide and 1-Ethyl-3-methylimidazoli um Ethylsulfate. Appl Spectrosc 61:1306–1311
37. Talaty ER, Raja S, Storhaug VJ, Dolle A, Carper WR (2004) Raman and Infrared Spectra and ab Initio Calculations of C_{2-4}MIM Imidazolium Hexafluorophosphate Ionic Liquids. J Phys Chem B 108:13177–13184
38. Reinert L, Batouche K, Leveque JM, Muller F, Beny JM, Kebabi B, Duclaux L (2012) Adsorption of imidazolium and pyridinium ionic liquids onto montmorillonite: characterization and thermodynamic calculations. Chem Eng J 209:13–19
39. Deepa M, Agnihotry SA, Gupta D, Chandra R (2004) Ion-pairing effects and ion-solvent-polymer interactions in $LiN(CF_3SO_2)_2$-PC-PMMA electrolytes: a FTIR study Electrochim Acta, 49:373–383
40. Chen HW, Chiu CY, Chang FC (2002) Conductivity enhancement mechanism of the poly(ethylene oxide)/modified-clay/$LiClO_4$ systems. J Polym Sci Pol Phys 40:1342–1353
41. Pandey GP, Agrawal RC, Hashmi SA (2011) Magnesium ion conducting gel polymer electrolytes dispersed with fumed silica for rechargeable magnesium battery application. J Solid State Electrochem 15:2253–2264
42. Jayanthi S (2019) Studies on ionic liquid incorporated polymer blend electrolytes for energy storage applications Adv Compos Hybrid Mater 2:351–360
43. Saroj AL, Singh RK (2012) Thermal, dielectric and conductivity studies on PVA/Ionic liquid [EMIM][$EtSO_4$] based polymer electrolytes. J Phys Chem Solids 73:162–168
44. Stepniak I, Andrzejewska E (2009) Highly conductive ionic liquid based ternary polymer electrolytes obtained by in situ photopolymerisation. Electrochim Acta 54:5660–5665
45. Mishra R, Rao KJ (1998) Electrical conductivity studies of poly(ethyleneoxi de)-poly(vinylalcohol) blends. Solid State Ion 106:113–127
46. Adachi K, Urakawa O (2002) Dielectric study of concentration fluctuations in concentrated polymer solutions. J Non-Cryst Solids 307–310:667–670
47. Liu J, Khanam Z, Muchakayala R, Song S (2020) Fabrication and characterization of Zn-ion-conducting solid polymer electrolyte films based on PVdF-HFP/Zn(Tf)2 complex system. J Mater Sci Mater Electron 31:6160–6173
48. Jie J, Liu Y, Cong L, Zhang B, Lu ZX, Liu J, Xie H, Sun L (2020) High-performance PVDF-HFP based gel polymer electrolyte with a safe solvent in Li metal polymer battery. J Energy Chem 49:80–88
49. Ghosh S, Ghosh A (2002) Conductivity relaxation in mixed alkali fluoride glasses. J Phys: Condens Matter 14:2531–2544
50. Dhahri Ah, Dhahri E, Hlil EK (2018) Electrical conductivity and dielectric behavior of nanocrystalline $La_{0.6}Gd_{0.1}Sr_{0.3}Mn_{0.75}Si_{0.25}O_3$ RSC Adv. 8:9103–9111
51. Hannan M, Hoque M, Mohamed A, Ayob A (2017) Review of energy storage systems for electric vehicle applications: issues and challenges Renew. Sustain Energy Reviews 69:771–789
52. Rhaiem AB, Chouaib S, Guidara K (2010) Dielectric relaxation and ionic conductivity studies of $Ag_2ZnP_2O_7$. Ionics 16:455–463
53. Komine S (2007) Dielectric relaxation study on $Ce_{0.9}Gd_{0.1}O_{1.95}$ ceramics. Physica B: Condens Matter 392:348–352
54. Jiya IN, Gurusinghe N, Gouws R (2018) Hybridization of Battery, Supercapacitor and Hybrid Capacitor for Electric Vehicles. 2018 IEEE PES/IAS Power Africa https://doi.org/10.1109/PowerAfrica.2018.8520991